[Frontiers in Bioscience E2, 752-763, January 1, 2010]

AtTFC B is involved in control of cell division

Yunlong Du[1], Meiqiang Cui[1], Dan Qian[1], Lei Zhu[3], Chunhong Wei[1], Ming Yuan[3], Zhongkai Zhang[4] and Yi Li[1, 2]

[1]Peking-Yale Joint Center for Plant Molecular Genetics and Agrobiotechnology, National Laboratory of Protein Engineering and Plant Genetic Engineering, College of Life Science, The National Plant Gene Research Center, Peking University, Beijing 100871, China, [2]National Center for Plant Gene Research, Beijing 100101, China, [3]State Key Laboratory of Plant Physiology and Biochemistry, Department of Plant Sciences, College of Biological Sciences, China Agricultural University, Beijing 100094, China, [4]Yunnan Provincial Key Laboratory of Agri-Biotechnology, Biotechnology and Genetic Resources Institute, Yunnan Academy of Agricultural Sciences, Kunming 650223, Yunnan, China

TABLE OF CONTENTS

1. ABSTRACT

Tubulin-folding cofactors play important roles in regulating plant development. Arabidopsis tubulin-folding cofactor B (AtTFC B) is an Arabidopsis homolog of mammalian tubulin-folding cofactor B, whose biological function in plant development remains poorly understood. Here we report that the homozygous *attfc b* (-/-) allele caused embryonic lethality. Embryogenesis was arrested at early embryo stage and the cells contained one or multiple nuclei. Plants carrying a heterozygous *attfc b* (+/-) allele exhibited enlarged mesophyll cells and leaf epidermal cells with bulged nuclei. Flow cytometry analysis showed increased ploidy in the leaves of the *attfc b* (+/-) mutant, as well as increased levels of *Cdc2A* and *CycB1;1*. In addition, immunofluorescence assay showed increased numbers of spindles and phragmoplasts in the *attfc b* (+/-) mutant. These results suggest that AtTFC B plays an important role in plant cell division.

2. INTRODUCTION

Microtubules control fundamental cellular processes, such as intracellular transport, cell division, cell expansion, cell polarity, and chromosome segregation. During cell cycle, plant cells display four kinds of microtubule arrays: the interphase cortical microtubule array, the preprophase band (PPB), the mitotic spindle, and the phragmoplast (1). Microtubules contain highly conserved alpha/beta-tubulin heterodimers, and different proteins are involved in the tubulin biogenesis, such as phosducin-like proteins required for beta-tubulin biogenesis (2, 3). The biogenesis of tubulin is a symmetrical process. First, the nascent alpha- and beta-polypeptide chains are captured and partially folded by prefoldin and chaperonins (4, 5). After release from the prefoldin and chaperonins, the partially folded alpha- and beta-tubulin chains are captured by tubulin-folding cofactors B and A, respectively. These cofactors are subsequently replaced by cofactors E and D,

respectively, and form a quaternary complex containing alpha-tubulin/E and beta-tubulin/D. When cofactor C binds to the quaternary complex, the cofactors C, D, and E act as a GTPase-activating protein (GAP), triggering hydrolysis of GTP by beta-tubulin to release alpha/beta-tubulin heterodimers (6, 7).

Tubulin-folding cofactors not only regulate the folding of tubulin heterodimers, but are also involved in the regulation of cell division associated with microtubule function. In fission yeast, the *alp1* and *sto1* alleles, which encode the homologs of cofactor D and E, respectively, disturb the microtubule structure leading to condensed chromosomes or unequal segregation and mitotic division defects (8-11). In Arabidopsis, KIESEL (KIS) and PORCINO (POR), the orthologs of cofactor A and C, respectively, are required for the synthesis of microtubules; mutations in these two genes cause cell division defects (12, 13). Mutation in TITAN1 (TTN1), the ortholog of cofactor D, results in cell division defect attributable to the disruption of microtubule function and endosperm with condensed chromosomes (14, 15). The *PILZ* group genes include *POR*, *CHO*, and *PFIFFERLING* (*PFI*), which encode the Arabidopsis orthologs of tubulin-folding cofactors C, D, and E, respectively (16). In *pilz* mutants, embryos show an absence of microtubule arrays and condensed chromosomes (16). Although mitotic division and cytokinesis are disturbed, the process of cell cycle is not affected in the *pilz* mutants (16, 17).

The function of tubulin-folding cofactor B is dependent on microtubules. In most cases, mammalian cofactor B is considered as a reservoir to sequester and deliver the alpha-tubulin folding intermediate to cofactor E (18). However, cofactor B is also important to microtubule polymerization in mammalian cells. Overexpression of cofactor B can depolymerize microtubules (19-22). Mutation in Alp11, a fission yeast homolog of cofactor B, destroyed microtubule structure and delayed mitosis with condensed chromosomes (23, 24), and is also essential for cell viability in fission yeast (23, 24). Overexpression of Alf1, a budding yeast ortholog of mammalian cofactor B, caused depolymerization of microtubules; however, Alf1 is not essential for cell survival in budding yeast (25). Different roles of cofactor B in different species suggest a complexity of its function. AtTFC B (AT3G10220) is the Arabidopsis homolog of mammalian cofactor B (17), and it can interact with alpha-tubulin *in vivo*. Overexpression of *AtTFC B* in cowpea protoplasts reduced the number of microtubules (26). However, the function of *AtTFC B* in plant development remains unknown.

Here, we provide evidence that AtTFC B is essential for embryogenesis in Arabidopsis. Cellular and molecular data indicate that AtTFC B is also involved in the regulation of post-embryonic development. Our data suggest that AtTFC B is required for cell division.

3. MATERIALS AND METHODS

3.1. Plant growth, mutant screening, and plant transformation

All Arabidopsis materials used in this study are in the Columbia (Col) background. The T-DNA insertion lines *attfc b* (+/-) (SALK-019471) and *attfc b-2* (SALK-002231) were obtained from the Arabidopsis Biological Resource Center (ABRC, Columbus, OH). Seeds were surface-sterilized with 10% sodium hypochlorite, sown on Murashige and Skoog medium (27) supplemented with 0.8% agar and 3% sucrose, and cold-treated for one day at 4°C. Seedlings were then grown in the medium under a 16 h light photoperiod at 21°C. Adult plants were grown in environmental chambers under a 16 h photoperiod at 21°C.

We genotyped the *attfc b* (+/-) mutant plants by PCR using the following specific primers, LBa1 (5'-T G G T T C A C G T A G T G G G C C A T C G-3'), BLP (5'-T G G C T T A C A T T T G C A G G G T G A A-3'), and BRP (5'-G G T C T T C G G G T T G T C G C T C T T-3') designed from SALK (http://signal.salk.edu/tdnaprimers.2.html).

To generate transgenic plants ectopically expressing *AtTFC B*, we cloned the coding sequence of *AtTFC B* into the modified plasmid pCambia3301 under the control of CaMV *35S* promoter, and transformed the construct into wild-type and *attfc b* (+/-) mutant plants using the floral dip method (28).

3.2. Cloning of *AtTFC B* coding sequence

Total RNA from wild-type Arabidopsis was extracted with RNeasy® Plant Mini kit (QIAGEN, Valencia CA). To obtain the first strand cDNA of the *AtTFC B* (AT3G10220) gene, total mRNA was used as a template for reverse transcription reaction with oligo-dT_{18} and SuperScript II™ RNase H-Reverse Transcriptase (Invitrogen, CA). The primers BFP (5'-C A C C C A T A T G A T G G C A A C T T C G C G T T T A C A G T T G-3') and BRP2 (5'-C G C G G A T C C T T A T A T T T C A T C T T C C T C G A A A G G-3') were used for RT-PCR. The purified PCR products were cloned into pENTR/D vector (Invitrogen, CA) following the manufacturer's instructions and confirmed by DNA sequencing.

3.3. Quantitative real-time PCR

To determine the expression levels of *AtTFC B*, *Cdc2A*, and *CycB1;1*, total RNA was isolated from different tissues using the RNA plant kit (Tiangen Biotech, Beijing). The RNA was quantified three times for each sample. To produce the first strand cDNA, 2 μg of total RNA pretreated with DNAase I (Promega, Madison, WI) was used as a template in reverse transcription reaction. At the end of the reaction, the cDNA was diluted with sterile distilled water. Real-time PCR was performed using the SYBR green-I qPCR kit (Finnzymes Oy), Fifty nanograms of the diluted cDNA and 0.75 pM gene-specific primers BFP450 (5'-C T A T A T G G A A G A T C T C T G C G C-3') and BRP732 (5'-T T A T A T T T C A T C T T C C T C G A A A G G-3'), Cdc2A FP (5'-A T G G G A A C T C C G T A C G A G G A T A C -3') and Cdc2A RP (5'-C T A A G G C A T G C C T C C A A G A T C C T T G-3'), CycB1;1 FP (5'-C T C A A G C A T C A C A C T G G C T A T T C-3') and CycB1;1 RP (5'-C T A A G C A G A T T C A G T T C C G G T C A A C-3') were used to amplify the *AtTFC B*, *Cdc2A* and *CycB1;1*, respectively, using the

DNA Engine Opticon™ 2 machine (Bio-Rad, CA, USA). The *Ubiquitin10* gene served as an internal control using specific primers UBQ10FP (5'-G A T C T T T G C C G G A A A A C A A T T G G A G G A T G G T-3') and UBQ10RP (5'-C G A C T T G T C A T T A G A A A G A A A G A G A T A A C A G G-3'). PCR conditions were as follows: 5 min at 94°C for the first denaturation step, 40 cycles followed with 10 s at 94°C, 20 s at 60°C, and 20 s at 72°C. Fluorescence of the PCR products was measured twice at the end of the extension step at 72°C and 84°C. Relative transcript levels of *AtTFC B*, *Cdc2A*, and *CycB1;1* were calculated using the following equation: $RE=2^{-\Delta\Delta Ct}$. For wild-type and *attfc b* (+/-) mutant plants, samples from three different individuals were measured.

3.4. Examination of ovules

Siliques at different developmental stages were harvested and dissected in Hoyer's solution (7.5 g of arabic gum, 100 g of trichloroacetaldehyde hydrate, and 5 mL of glycerol diluted with water to 100 mL) under a stereomicroscope. The ovules were examined immediately under a Zeiss Axioskop2 plus Microscope and digital images were acquired using Carl Zeiss imaging systems (Carl Zeiss, Jena, Germany).

3.5. Leaf morphology and structure

Leaf epidermal cells were examined with a Field Emission Environmental Scanning Electron Microscopy (model QUANTA 200F, FEI, OR). To study the mesophyll structure, leaves were fixed overnight in a solution of 3% glutaraldehyde (Sigma-Aldrich, St. Louis, MO), washed, dehydrated in a series of ethanol, and embedded in LR White resin (London Resin Co., London, United Kingdom). Five micrometer-thick sections were obtained with a glass knife on a microtome (Model 1512, Leitz), mounted onto slides, and stained with 0.1% (w/v) toluidine blue-O. The slides were examined with a Leica microscope (Type 020-525.025, Leica Microsystems, Wetzlar, Germany) and photographed with KX Series Imaging System (Model KX32E, Apogee Instruments Inc., Roseville, CA). The nuclei of leaf epidermal cells were detected as previously described by Boudolf and his colleagues (29). The nuclei and cell sizes of leaf epidermal cells and mesophyll cells were measured using Image J 1.36b software (NIH, Bethesda, MD).

3.6. Analysis of microtubule

Microtubule arrays were detected in roots based on previously described (30). The root tips were dissected from seven-day-old seedlings grown under light conditions and fixed in 4% (v/v) paraformaldehyde. For immunolabeling, the root samples were first incubated with a mouse anti-alpha-tubulin monoclonal antibody (Sigma-Aldrich) at a 1:200 dilution, washed and then incubated with FITC-conjugated goat anti-mouse IgG (Molecular Probes, Eugene, OR) at a 1:500 dilution. The samples were examined under a Leica fluorescence microscope (Type 020-525.025, Leica Microsystems, Wetzlar, Germany).

3.7. Flow cytometry

The third leaf was chopped with a razor blade in 0.5 mL of cold Galbraith buffer (31). The extracts were filtered through a 60 μm pre-wet nylon mesh and collected in a 1.5 mL eppendorf tube. The filtrate was incubated with 10 μL of 10 mg/mL RNaseA for 20 min at 37°C, and then stained with 2 μL of 5 mg/mL propidium iodide (Sigma-Aldrich) and gently dispersed the nuclei. The sample was kept at 4°C in dark conditions for 10 min. Approximately 3500-5500 nuclei were analyzed with FACS Calibur flow cytometer, and DNA histograms and proportions were generated using Cellquest software (Becton, Dickinson and Company, Franklin Lakes, NJ).

3.8. Statistical analyses

Data were analyzed using student *t*-test for statistical significance and all images were processed with Photoshop™ 7.0.1 (Adobe Systems Inc., San Jose, CA).

4. RESULTS

4.1. The homozygous *attfc b* (-/-) allele caused embryonic lethality

To understand the function of AtTFC B in plant development, a T-DNA insertion line (SALK-019471) was obtained from ABRC (Figure 1A). The T-DNA was inserted at position +1846 of the 3' region of *AtTFC B* genomic sequence (Figure 1B). To test if this insertion affects transcription of *AtTFC B* gene, the level of *AtTFC B* mRNA was determined using quantitative real-time PCR. As shown in Figure 1C, *AtTFC B* mRNA expression was reduced in the roots, stems, leaves and siliques in the T-DNA insertion line.

In screening for *attfc b* mutant plants, only heterozygous mutant plants were obtained in this T-DNA insertion line (Figure 1D). Progeny analysis using the X^2 test for heterozygous *attfc b* (+/-) plants showed a segregation ratio of 1:2 for wild-type (n = 188) to heterozygous plants (n = 321), suggesting the potential embryo lethality of the homozygous *attfc b* (-/-) plants. To test this hypothesis, we examined the phenotypes of the embryos using differential interference contrast microscope. In contrast to the wild-type embryos (Figures 2A, 2C, 2E and 2G), approximately 20% of mutant embryos were arrested at early two or four cells developmental stage, carrying multiple nuclei (Figures 2B, 2D, 2F and 2H). Given the possibility that some embryos may have stopped development or degenerated at an earlier stage, the percentage of defective embryos was close to what was expected for *attfc b* (-/-) genotype.

4.2. Plants carrying a heterozygous *attfc b* (+/-) allele had enlarged cell size

To test whether AtTFC B plays a role in plant growth beyond embryogenesis, we examined the phenotypes of heterozygous *attfc b* (+/-) plants. Heterozygous plants had different phenotypes from the wild-type: the plants were taller with bigger rosettes (Figures 3A, 3B), and the third true leaf was significantly longer and wider (Figure 3C) (Table 1). Consistent with enlarged leaf, the mesophyll cells in *attfc b* (+/-) mutant were significantly larger than those in the wild-type (Figures 3D, 3E; Table 1). We found that the leaf epidermal cells of *attfc b* (+/-) mutant were also larger than those in

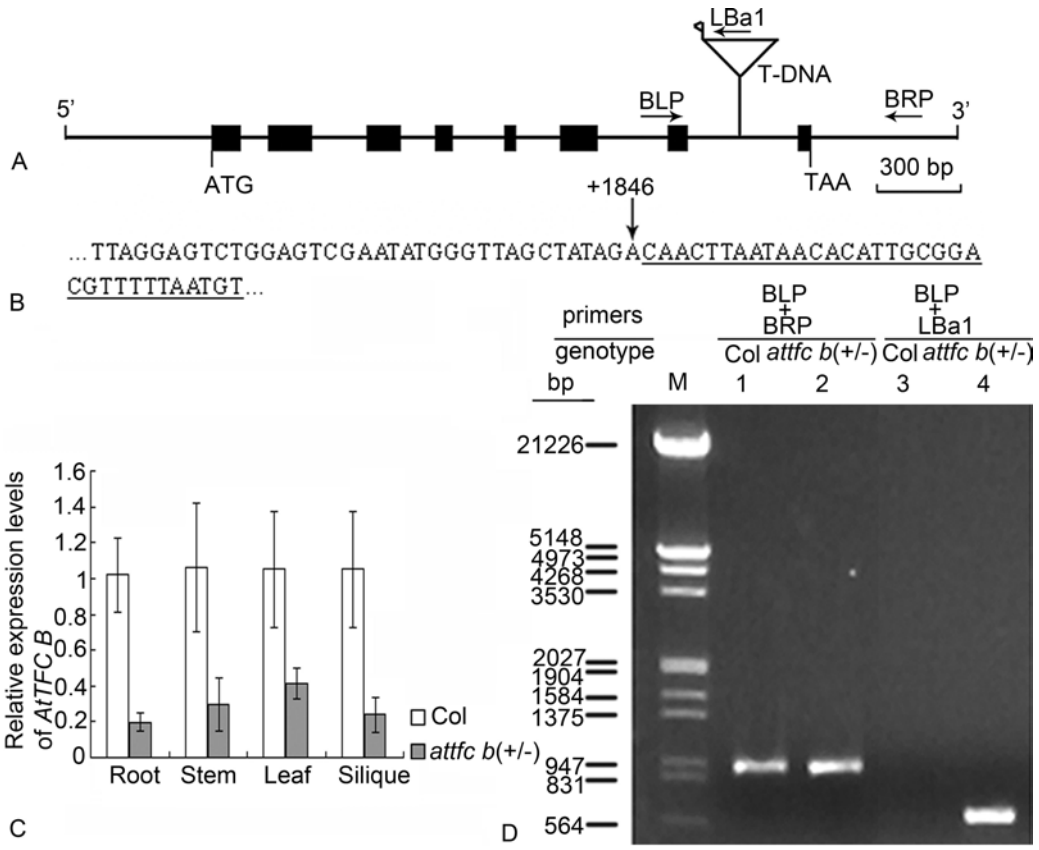

Figure 1. T-DNA insertion line and the expression profiles of *AtTFC B*. (A) A T-DNA is inserted in the 3' region of the *AtTFC B* genomic sequence in the *attfc b* (+/-) mutant. The open arrowhead indicates the left border of the T-DNA. Solid rectangles denote exons and the horizontal lines indicate the 5' leader, 3' trailer, and introns. The arrows indicate the positions of the BLP, BRP, and LBa1 primers. (B) The nucleotide position of T-DNA insertion site. One T-DNA is inserted at the +1846 position of the *AtTFC B* genomic sequence. The underlined nucleotides represent the T-DNA sequence. The *AtTFC B* genomic sequence is derived from the MIPS database (http://mips.gsf.de/proj/thal/db/index.html). (C) Relative expression levels of *AtTFC B* in different organs of wild-type and *attfc b* (+/-) plants. The accumulation levels of *AtTFC B* mRNA in different organs were reduced in *attfc b* (+/-) plants, as determined by quantitative real-time PCR. Each dataset represents the average from three biological replicates plus the standard error. (D) Genotyping of *attfc b* (+/-) mutant plants by PCR. Using gene-specific primers BLP and BRP for *AtTFC B*, and a T-DNA-specific primer LBa1, the PCR results confirmed a T-DNA insertion in the *attfc b* (+/-) plant as shown in (A). Col = Wild-type. M = λ DNA /*Eco*RI+*Hin*dIII molecular weight marker.

the wild-type (Figures 4A, 4B). The axial length in the mutant (52.2 μm) was significantly longer than that of the wild-type (44.8 μm) (Table 1), and the leaf epidermal cells contained enlarged nuclei (Figure 4D, Table 1).

To confirm that mutations in *AtTFC B* caused leaf morphological defects, we analyzed the phenotype of another *attfc b* mutant (SALK-002231) named *attfc b-2*. The *attfc b-2* mutant also exhibited enlarged leaf sizes (Figure 5). These results indicate that AtTFC B play an important role in post-embryonic growth in Arabidopsis.

4.3. Overexpression of *AtTFC B* restored the *attfc b* (+/-) phenotype and inhibited growth in the wild-type background

We further tested if the expression of *AtTFC B* in *attfc b* (+/-) mutant background would rescue the *attfc b* mutant phenotype. We expressed the *AtTFC B* coding sequence (CDS) under the control of CaMV *35S* promoter (Figure 6A). Phenotypic analysis showed that the expression of *AtTFC B* restored *attfc b* (+/-) phenotype to the wild-type phenotype (Figures 6B, 6C, Table 2).

The phenotypes of *attfc b* (+/-) plants suggested that AtTFC B functions to inhibit cell and organ growth in post-embryonic development. In this scenario, we would expect that overexpression of *AtTFC B* in the wild-type background would lead to inhibition of plant growth. Indeed, overexpression of *AtTFC B* in the wild-type background displayed reduction in both rosette size and leaf size (Figures 6B, 6D, Table 2).

4.4. Mutation in *AtTFC B* altered ploidy levels and mRNA levels of *Cyclin B1;1* and *Cdc2A*

Homozygous *attfc b* (-/-) embryos displayed impaired nuclear division (Figures 2B, 2D, 2F, 2H) and the heterozygous *attfc b* (+/-) plants showed enlarged nuclei in leaf epidermal cells (Figure 4D). To further test the

Table 1. Statistics of leaf structural measured in wild type and *attfc b* (+/-) mutant plants

Plant lines	Rosette diameter (cm)	Leaves		Leaf epidermal cells		Mesophyll cells
		Length(mm)	Width(mm)	Axial length (μm)	Nucleus area (μm^2)	Cell area(μm^2)
Wild type	3.3 +/- 1.0 (n = 38)	4.5 +/- 1.3 (n = 26)	3.0 +/- 0.8 (n = 26)	44.8 +/- 10.3 (n = 56)	38.0 +/- 12.5 (n = 417)	1294.0 +/- 1048.7 (n = 291)
attfc b (+/-)	5.1 +/- 1.3[1] (n = 34)	6.1 +/- 1.7[1] (n = 25)	3.8 +/- 0.8[1] (n = 25)	52.2 +/- 10.7[1] (n = 62)	52.1 +/-20.6[1] (n = 393)	1602.4 +/- 1260.8[1] (n = 314)

Rosettes of three-week-old seedlings, leaves of two-week-old seedlings, and nuclei of leaf epidermal cells in three-week-old seedlings were examined. All data represent means and standard deviation, n = number of samples measured. [1]T-test shows statistically significant differences between wild type and *attfc b* (+/-) mutant plants, and *P* value is less than 0.01.

Table 2. Sizes of rosettes and leaves from wild-type, rescued *attfc b* (+/-), and *AtTFC B*-overexpression plants

Plant lines	Rosette diameter (cm)	Leaf length (mm)	Leaf width (mm)
Wild type	3.5 +/- 0.9 (n = 43)	4.1 +/- 1.2 (n = 34)	3.4 +/- 0.9 (n = 34)
RB12[1]	3.5 +/- 0.8 (n = 30)	3.7 +/- 0.9 (n = 30)	3.2 +/- 0.9 (n = 30)
OB13[2]	3.0 +/- 0.5[3] (n = 18)	3.0 +/- 0.9[3] (n = 20)	2.4 +/- 0.8[3] (n =20)

Rosettes of three-week-old seedlings and leaves of two-week-old seedlings were measured. All data represent means and standard deviation. n = number of samples measured. [1]Rescued *attfc b* (+/-) mutant line 12. [2]*AtTFC B*-overexpression line 13. [3]T-test shows statistically significant differences between wild-type and *AtTFC B*-overexpression plants, and *P* value is less than 0.01.

Table 3. DNA polyploidy levels in leaves of wild-type, *attfc b* (+/-) mutant, and *AtTFC B*-overexpression plants.

Plant lines	2C (%)	4C (%)	8C (%)	16C (%)	32C (%)
Wild type (n = 5)	34.7 +/- 4.5	54.7 +/- 3.4	6.5 +/- 1.3	0.37 +/- 0.20	
attfc b (+/-) (n = 5)	15.1 +/- 1.1	45.4 +/- 9.2	32.9 +/- 9.1	2.01 +/- 0.84	0.13 +/- 0.08
OB13[1] (n = 3)	29.8 +/- 3.9	59.4 +/- 2.1	6.1 +/- 4.1	0.33 +/- 0.21	

Leaves of 21 DAG seedlings grown under a 16 h photoperiod were analyzed with flow cytometry. For each sample, 3 500-5 500 nuclei were analyzed for their ploidy levels. All data represent means and standard deviation. [1] *AtTFC B*-overexpression line 13. n = number of samples examined.

Table 4. Percentages of the four-microtubule arrays in root tip cells of wild-type and *attfc b* (+/-) mutant plants

Cell lines	Cortical microtubule	Preprophase band	Spindle	Phragmoplast
Wild type (n = 1565)	93.7%	4.0%	1.0%	1.3%
attfc b (+/-) (n = 1855)	92.3%	4.1%	1.3%	2.3%

Seven-day-old seedlings that grew under a 16 h photoperiod were used to observe microtubule arrays. The microtubule arrays in root tip cells of over 80 roots from each line were studied by confocal microscopy. n = number of cells examined.

karyokinesis defect in the *attfc b* mutant, we measured DNA ploidy levels in the leaves of 21-day-old *attfc b* (+/-) mutants, *AtTFC B*-overexpressing plants and wild-type plants leaves using flow cytometry analysis. In contrast to the 1.6-fold increase observed in the ratio of 4C leaf cells to 2C leaf cells in wild-type (2C = 34.7% and 4C = 54.7%), there was an approximately 3-fold increase in the *attfc b* (+/-) mutant (2C = 15.1% and 4C = 45.4%) (Figures 7A, 7B, Table 3). Furthermore, mutation in *AtTFC B* increased the polyploidy levels. The fraction of 8C and 16C cells significantly increased in the *attfc b* (+/-) mutant leaf cells (Figure 7B, Table 3). It also had a small fraction of 32C cells (0.13%) that was absent from the wild-type leaf cells (Figures 7A, 7B, Table 3). However, the fraction of 8C and 16C cells were slightly decreased in the *AtTFC B*-overexpressing plants compared with the wild-type (Figure 7C, Table 3).

In the *pilz* group mutants, GUS staining of embryos revealed the expression of *Cdc2A* and *CycB1;1* (16). To determine if these two genes were affected in *attfc b* (+/-) mutant and *AtTFC B*–overexpressing plants, we analyzed the levels of *CyclinB1;1* and *Cdc2A* mRNA. Consistent with the ploidy level, the levels of *Cdc2A* and *CycB1;1* mRNA were upregulated in *attfc b* (+/-) mutant and reduced in *AtTFC B* transgenic plants (Figure 8).

4.5. Microtubule arrays were affected in the *attfc b* (+/-) mutant

We further tested if microtubule arrays were affected in the *attfc b* (+/-) mutant. We performed immunostaining for alpha-tubulin in root tip cells of *attfc b* (+/-) mutant and the wild-type. As shown in Table 4, the percentage of spindle and phragmoplasts in *attfc b* (+/-) mutant increased by 30% and 77%, respectively, relative to the wild-type. The PPB was slightly increased (2.5%) and the cortical microtubule arrays were reduced (1.5%) in the *attfc b* (+/-) mutant compared with those in wild-type plants (Table 4). These data suggested that cytokinesis might be defective in the *attfc b* (+/-) mutant.

5. DISCUSSION

Tubulin-folding cofactors are involved in the control of cell division. In this study, we showed that AtTFC B, the homolog of mammalian cofactor B, is

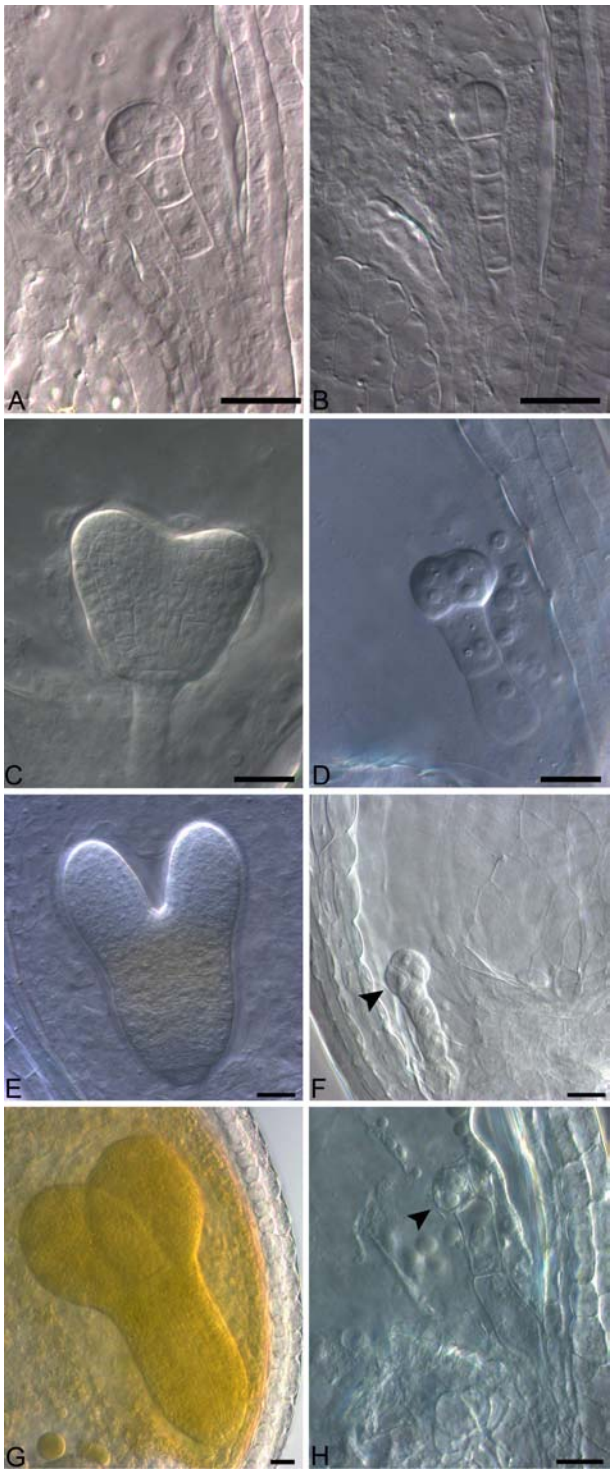

Figure 2. Embryo development in wild type and *attfc b* (-/-) mutant plants. (A) and (B) Early-stage embryo. Embryos are shown in wild type (A) and the *attfc b* (-/-) mutant (B). Scale bar = 20 μm. (C) and (D) Early heart-stage embryos. The *attfc b* (-/-) embryo (D) is arrested at the early stage embryo in contrast to the wild-type plant (C). The *attfc b* (-/-) embryo has four cells, each containing more nuclei. Scale bar = 20 μm. (E) and (F) Torpedo-stage embryo. The *attfc b* (-/-) embryo (F) still remains at the early stage embryo in contrast to that of the wild-type plant (E). The arrowhead indicates the embryo. Scale bar = 20 μm. (G) and (H) Mature embryos. The *attfc b* (-/-) embryo (H) remains arrested at the four-cell stage, with each cell containing one or more nuclei, compared with that of the wild-type plant (G). The arrowhead indicates the embryo. Scale bar = 20 μm.

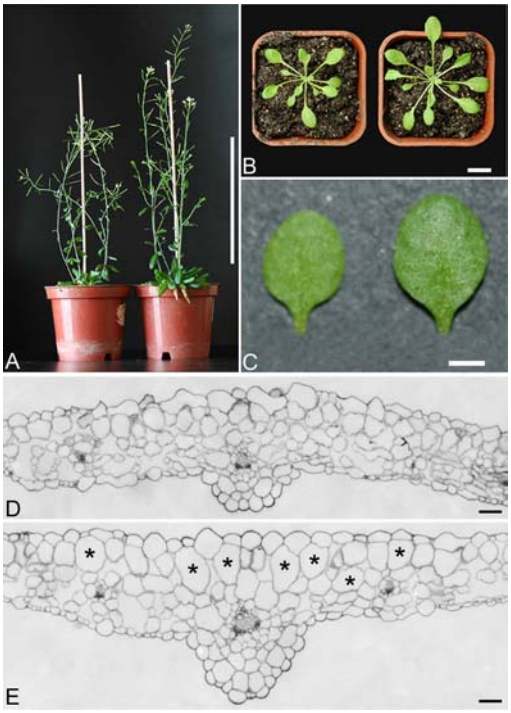

Figure 3. Growth heights and leaf structures in wild-type and *attfc b* (+/-) mutant plants. (A) Morphogenesis of nine-week-old plants. *attfc b* (+/-) mutant plants (right) are taller than wild-type plants (left). Scale bar = 10 cm. (B) Three-week-old rosettes of wild-type (left) and *attfc b* (+/-) mutant (right) plants. The mutant plant is larger than the wild-type. Scale bar = 10 mm. (C) The third leaves from 14-day-old wild-type (left) and *attfc b* (+/-) mutant plants (right). The mutant leaf is longer and wider than the wild-type. Scale bar = 2 mm. (D) and (E) Transverse sections of leaves showing mesophyll cells in wild-type (D) and *attfc b* (+/-) mutant (E) plants. Asterisks point to some enlarged mesophyll cells in the *attfc b* (+/-) mutant plants. Scale bar = 50 μm.

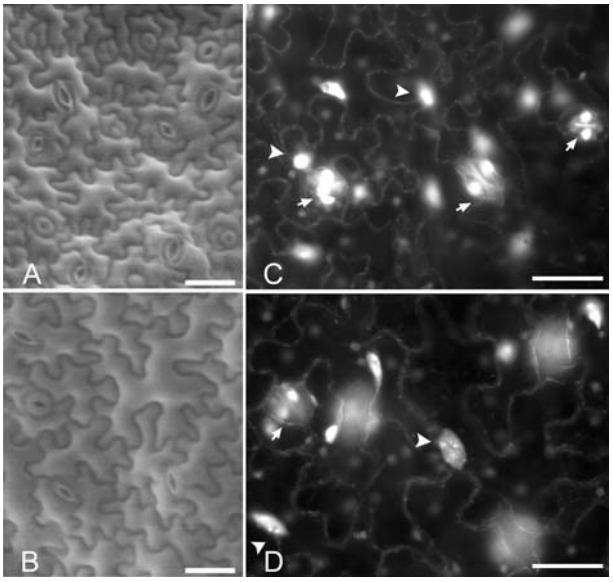

Figure 4. Nucleus morphogenesis of leaf epidermal cells in wild-type and *attfc b* (+/-) mutant plants. (A) and (B) Leaf epidermal cells in 14-day-old wild-type (A) and *attfc b* (+/-) mutant plants (B). The mutant plant has enlarged epidermal cells. Scale bar = 25 μm. (C) and (D) Nucleus phenotypes in 21-day-old wild-type (C) and *attfc b* (+/-) mutant plants (D). Nucleus was stained with DAPI. The mutant plant has bulged nuclei in the leaf epidermal cells. An arrow head points to the nucleus of leaf epidermal cells, and an arrow shows the nucleus of guard cells. Scale bar = 25 μm.

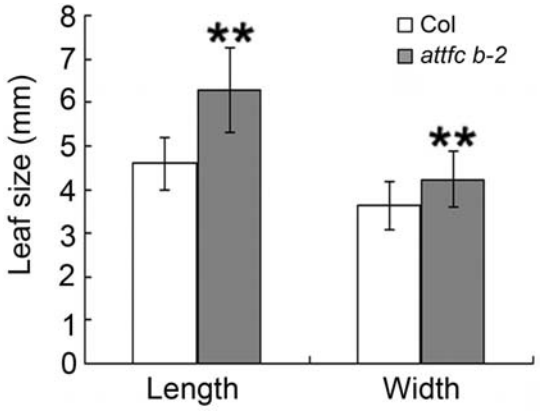

Figure 5. Leaf size in *attfc b-2* mutant plants. The leaf length of the *attfc b-2* (6.3 +/- 1.0 mm, n = 43) was longer than that of the wild-type plants (4.6 +/- 0.6 mm, n = 22), and the leaf width of *attfc b-2* (4.2 +/- 0.7 mm, n = 43) was also wider than wild-type plants (3.6 +/- 0.5 mm, n = 22). Col = Wild-type. Asterisks showed statistically significant differences between *attfc b-2* and wild-type (*t*-test, *P* value is less than 0.01). Bars represent the standard deviation.

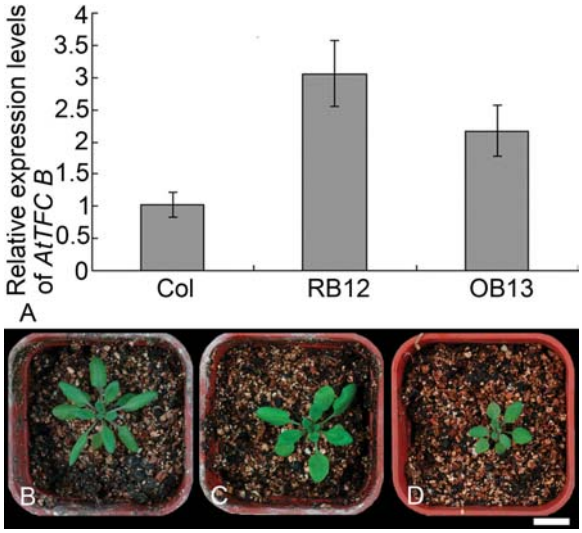

Figure 6. Effects of ectopic *AtTFC B* expression on the growth of *attfc b* (+/-) and wild-type plants. (A) The expression levels of *AtTFC B* mRNA in the rescued *attfc b* (+/-) mutant and *AtTFC B*-overexpression plants. *AtTFC B* coding sequence (CDS) under the control of CaMV *35S* promoter was transformed into the *attfc b* (+/-) mutant and wild-type background, respectively, to obtain the rescued *attfc b* (+/-) mutant and *AtTFC B*-overexpression transgenic plants. Each dataset represents the average of three independent experiments plus the standard deviation. Col = Wild-type. RB12 = Rescued *attfc b* (+/-) mutant line 12. OB13 = *AtTFC B*-overexpression transgenic line 13. (B) Rosettes of three-week-old wild-type plant. Scale bar = 10 mm. (C) Rosettes of three-week-old rescued *attfc b* (+/-) mutant line 12. The rescued plant shows a similar morphology to that of the wild-type plant (B). Scale bar = 10 mm. (D) Rosettes of three-week-old *AtTFC B*-overexpression transgenic line 13. The plant produce greatly reduced rosette compared with the wild-type (B). Scale bar = 10 mm.

required for cell division in Arabidopsis development. Specifically, embryos of homozygous *attfc b* (-/-) plants were arrested at early developmental stage and cells have multiple nuclei. In the *PILZ* group genes, mutant embryos contain varying numbers of nuclei and lack microtubules such as the spindle and phragmoplast (16, 17). Mutation in the *EDE1* gene caused defective endosperm, which was consistent with the absence of mitotic spindles and phragmoplasts (32). In the *attfc b* (+/-) mutant, the number of spindles and phragmoplasts was increased in root cells (Table 4). Given the direct role of the phragmoplast in the formation of new cell plate during cytokinesis (33), the possibility that the cytokinesis arrest resulted from the phragmoplast defect in the *attfc b* (-/-) mutant and caused improper cell division can not be excluded.

Besides cell division defect in embryogenesis, the heterozygous *attfc b* (+/-) mutant caused larger leaf epidermal cells (Figure 4B, Table 1), while *AtTFC B*-overexpressing plants were smaller in leaf size (Table 2). The distinct leaf phenotypes between *attfc b* (+/-) mutant and *AtTFC B*-overexpressing plants, suggest that AtTFC B

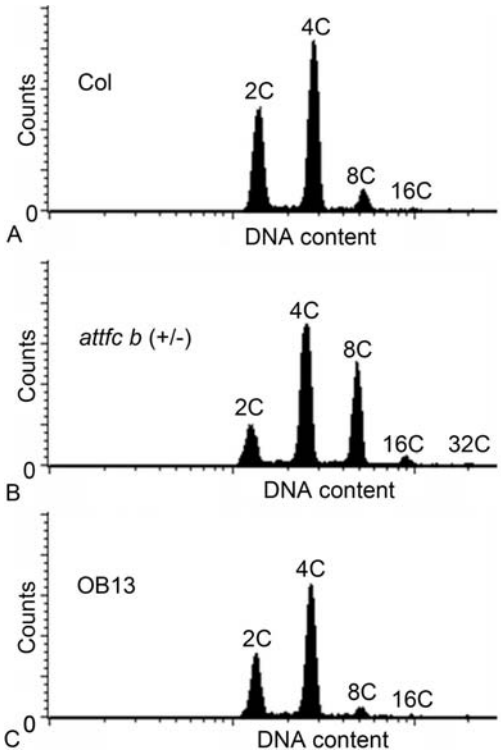

Figure 7. Ploidy levels in the leaves of wild-type, *attfc b* (+/-) mutant, and *AtTFC B*-overexpression plants measured by flow cytometry. The ploidy levels of the third leaves of 21-day-old plants are represented. The polyploidy levels were increased in the *attfc b* (+/-) mutant but reduced in *AtTFC B*-overexpression line 13, compared with those of wild-type. Col = Wild-type. OB13 = *AtTFC B*-overexpression line 13.

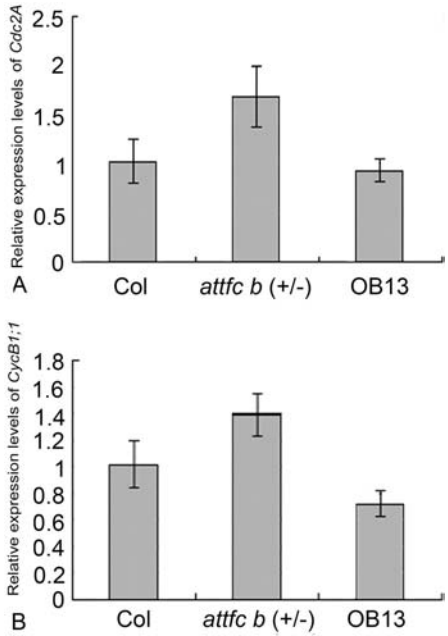

Figure 8. The expression levels of *Cdc2A* and *CycB1;1* in the *attfc b* (+/-) mutant and *AtTFC B*-overexpression plants. (A) The levels of *Cdc2A* were increased in the *attfc b* (+/-) mutant but decreased in *AtTFC B*-overexpression line OB13. (B) The levels of *CycB1;1* were increased in the *attfc b* (+/-) mutant but decreased in *AtTFC B*-overexpression line OB13. Each dataset represents the average of three independent experiments plus the standard deviation. Col = Wild-type. OB13 = *AtTFC B*-overexpression line 13.

functions as a negative regulator of cell division, at least in the post-embryonic organs.

Cell division is tightly related to cell cycle. Although function of tubulin-folding cofactors could affect cell division, the roles of tubulin-folding cofactors in cell cycle are different. Mammalian cells transfected with cofactor A siRNA were arrested at G1 phase (34), and overexpression of Alf1, the budding yeast homolog of cofactor B, arrested cell cycle causing defects in microtubule function (25). However, in *pilz* group mutant plants, cell cycle was not arrested even when mitotic division was arrested (16). In this study, the formation of PPB was still present in the root meristem cells (Table 4), indicating that G2-to-M transition point of the cell cycle was not arrested in *attfc b* (+/-) mutant. However, the number of phragmoplasts was obviously increased in *attfc b* (+/-) mutant (Table 4), suggesting that cell cycle might be arrested at the mitotic telophase, which resulted in cytokinesis defect.

Mutation of *AtTFC B* showed enlarged nuclei in leaf epidermal cells and was consistent with higher ploidy levels in the leaves (Figures 4D, 7B). A previous study showed that enhanced levels of a non-destructible *Cyclin B1* (also named *CycB1;1*) leads to doubled DNA content resulting from endomitosis. Weingartner and his colleagues concluded that the mitotic cyclins were required for reorganization of the phragmoplast and for proper cytokinesis (35). In this study, mutation in *AtTFC B* upregulated levels of *Cdc2A* and *CycB1;1* (Figure 8), as well as the number of phragmoplasts (Table 4). In contrast, overexpression of *AtTFC B* decreased the levels of *Cdc2A* and *CycB1;1* (Figure 8) and the polyploidy levels (Figure 7C). Thus, endomitosis might have occurred in *attfc b* (+/-) mutants when cytokinesis was disturbed. Mutation in *AtTFC B* also increased the number of spindles (Table 4), and increased mRNA levels of *Cdc2A* (Figure 8A). Cdc2 activity is required for microtubule recruitment. It is located at the nucleus and is associated with spindles and phragmoplasts during mitosis and cytokinesis (36). Taking these phenotypes into account, our data suggest that AtTFC B plays a critical role in ensuring a normal cell division process, and *AtTFC B* mutation might promote cells to enter into the process of endomitosis when cell division is arrested.

6. ACKNOWLEDGEMENTS

This project was supported by grants from the National Science Foundation of China and 985 programs to Yi. Li. We thank Professor Liying Du (Peking University) for assistance with the flow cytometry analysis. We thank Dr. Biao Ding (Ohio State University), Dr. Zhenbiao Yang (University of California, Riverside), Dr. Gang Wu (University of Pennsylvania) and Dr. Lieven De Veylder (Ghent University) for their critical reading and suggestions. We thank the Arabidopsis Biological Resource Center (Columbus, Ohio) for providing the *attfc b* (+/-) (SALK-019471) and *attfc b-2* (SALK-002231) mutant plants.

7. REFERENCES

1. Chan, J., G. Calder, S. Fox and C. Lloyd: Localization of the microtubule end binding protein EB1 reveals alternative pathways of spindle development in Arabidopsis suspension cells. *Plant Cell*, 17, 1737-1748 (2005)

2. Stirling, P. C., J. Cuellar, G. A. Alfaro, F. El Khadali, C. T. Beh, J. M. Valpuesta, R. Melki and M. R. Leroux: PhLP3 modulates CCT-mediated actin and tubulin folding via ternary complexes with substrates. *J Biol Chem*, 281, 7012-7021 (2006)

3. Castellano, M. M. and R. Sablowski: Phosducin-Like Protein 3 is required for microtubule-dependent steps of cell division but not for meristem growth in Arabidopsis. *Plant Cell*, 20, 969-981 (2008)

4. Lewis, S. A., G. Tian, I. E. Vainberg and N. J. Cowan: Chaperonin-mediated folding of actin and tubulin. *J Cell Biol*, 132, 1-4 (1996)

5. Valpuesta, J. M., J. Martin-Benito, P. Gomez-Puertas, J. L. Carrascosa and K. R. Willison: Structure and function of a protein folding machine: the eukaryotic cytosolic chaperonin CCT. *FEBS Lett*, 529, 11-16 (2002)

6. Tian, G., A. Bhamidipati, N. J. Cowan and S. A. Lewis: Tubulin folding cofactors as GTPase-activating proteins. GTP hydrolysis and the assembly of the alpha/beta-tubulin heterodimer. *J Biol Chem*, 274, 24054-24058 (1999)

7. Szymanski, D.: Tubulin folding cofactors: half a dozen for a dimer. *Curr Biol*, 12, R767-769 (2002)

8. Fedyanina, O. S., A. J. Book and E. L. Grishchuk: Tubulin heterodimers remain functional for one cell cycle after the inactivation of tubulin-folding cofactor D in fission yeast cells. *Yeast*, 26, 235-247 (2009)

9. Hirata, D., H. Masuda, M. Eddison and T. Toda: Essential role of tubulin-folding cofactor D in microtubule assembly and its association with microtubules in fission yeast. *EMBO J*, 17, 658-666 (1998)

10. Grishchuk, E. L. and J. R. McIntosh: Sto1p, a fission yeast protein similar to tubulin folding cofactor E, plays an essential role in mitotic microtubule assembly. *J Cell Sci*, 112 1979-1988 (1999)

11. Fedyanina, O. S., P. V. Mardanov, E. M. Tokareva, J. R. McIntosh and E. L. Grishchuk: Chromosome segregation in fission yeast with mutations in the tubulin folding cofactor D. *Curr Genet*, 50, 281-294 (2006)

12. Kirik, V., P. E. Grini, J. Mathur, I. Klinkhammer, K. Adler, N. Bechtold, M. Herzog, J. M. Bonneville and M. Hulskamp: The Arabidopsis tubulin-folding cofactor A gene is involved in the control of the alpha/beta-tubulin monomer balance. *Plant Cell*, 14, 2265-2276 (2002)

13. Kirik, V., J. Mathur, P. E. Grini, I. Klinkhammer, K. Adler, N. Bechtold, M. Herzog, J. M. Bonneville and M. Hulskamp: Functional analysis of the tubulin-folding cofactor C in Arabidopsis thaliana. *Curr Biol*, 12, 1519-1523 (2002)

14. Liu, C. M. and D. W. Meinke: The titan mutants of Arabidopsis are disrupted in mitosis and cell cycle control during seed development. *Plant J*, 16, 21-31 (1998)

15. Tzafrir, I., J. A. McElver, C. M. Liu Cm, L. J. Yang, J. Q. Wu, A. Martinez, D. A. Patton and D. W. Meinke: Diversity of TITAN functions in Arabidopsis seed development. *Plant Physio*l, 128, 38-51 (2002)

16. Mayer, U., U. Herzog, F. Berger, D. Inze and G. Jurgens: Mutations in the pilz group genes disrupt the microtubule cytoskeleton and uncouple cell cycle progression from cell division in Arabidopsis embryo and endosperm. *Eur J Cell Biol*, 78, 100-108 (1999)

17. Steinborn, K., C. Maulbetsch, B. Priester, S. Trautmann, T. Pacher, B. Geiges, F. Kuttner, L. Lepiniec, Y. D. Stierhof, H. Schwarz, G. Jurgens and U. Mayer: The Arabidopsis PILZ group genes encode tubulin-folding cofactor orthologs required for cell division but not cell growth. *Genes Dev*, 16, 959-971 (2002)

18. Tian, G., S. A. Lewis, B. Feierbach, T. Stearns, H. Rommelaere, C. Ampe and N. J. Cowan: Tubulin subunits exist in an activated conformational state generated and maintained by protein cofactors. *J Cell Biol*, 138, 821-832 (1997)

19. Vadlamudi, R. K., C. J. Barnes, S. Rayala, F. Li, S. Balasenthil, S. Marcus, H. V. Goodson, A. A. Sahin and R. Kumar: p21-activated kinase 1 regulates microtubule dynamics by phosphorylating tubulin cofactor B. *Mol Cell Biol*, 25, 3726-3736 (2005)

20. Wang, W., J. Ding, E. Allen, P. Zhu, L. Zhang, H. Vogel and Y. Yang: Gigaxonin interacts with tubulin folding cofactor B and controls its degradation through the ubiquitin-proteasome pathway. *Curr Biol*, 15, 2050-2055 (2005)

21. Kortazar, D., M. L. Fanarraga, G. Carranza, J. Bellido, J. C. Villegas, J. Avila and J. C. Zabala: Role of cofactors B (TBCB) and E (TBCE) in tubulin heterodimer dissociation. *Exp Cell Res*, 313, 425-436 (2007)

22. Lopez-Fanarraga, M., G. Carranza, J. Bellido, D. Kortazar, J. C. Villegas and J. C. Zabala: Tubulin cofactor B plays a role in the neuronal growth cone. *J Neurochem*, 100, 1680-1687 (2007)

23. Radcliffe, P. A., D. Hirata, L. Vardy and T. Toda: Functional dissection and hierarchy of tubulin-folding cofactor homologues in fission yeast. *Mol Biol Cell*, 10, 2987-3001 (1999)

24. Radcliffe, P. A. and T. Toda: Characterisation of fission yeast alp11 mutants defines three functional domains within tubulin-folding cofactor B. *Mol Gen Genet*, 263, 752-760 (2000)

25. Feierbach, B., E. Nogales, K. H. Downing and T. Stearns: Alf1p, a CLIP-170 domain-containing protein, is functionally and physically associated with alpha-tubulin. *J Cell Biol*, 144, 113-124 (1999)

26. Dhonukshe, P., B. O. Bargmann and T. W. Gadella, Jr.: Arabidopsis tubulin folding cofactor B interacts with alpha-tubulin *in vivo*. *Plant Cell Physiol*, 47, 1406-1411 (2006)

27. Murashige, T. and F. Skoog: A revised medium for rapid growth and bioassays with tobacco tissue cultures. *Physiol Plant*, 15, 473-497 (1962)

28. Clough, S. J. and A. F. Bent: Floral dip: a simplified method for Agrobacterium-mediated transformation of Arabidopsis thaliana. *Plant J*, 16, 735-743 (1998)

29. Boudolf, V., K. Vlieghe, G. T. Beemster, Z. Magyar, J. A. Torres Acosta, S. Maes, E. Van Der Schueren, D. Inze and L. De Veylder: The plant-specific cyclin-dependent kinase CDKB1;1 and transcription factor E2Fa-DPa control the balance of mitotically dividing and endoreduplicating cells in Arabidopsis. Plant Cell, 16, 2683-2692 (2004)

30. Wang, X., L. Zhu, B. Liu, C. Wang, L. Jin, Q. Zhao and M. Yuan: Arabidopsis microtubule-associated protein 18 functions in directional cell growth by destabilizing cortical microtubules. *Plant Cell*, 19, 877-889 (2007)

31.Galbraith, D. W., K. R. Harkins, J. M. Maddox, N. M. Ayres, D. P. Sharma and E. Firoozabady: Rapid flow cytometric analysis of the cell cycle in intact plant tissues. *Science*, 220, 1049-1051 (1983)

32. Pignocchi, C., G. E. Minns, N. Nesi, R. Koumproglou, G. Kitsios, C. Benning, C. W. Lloyd, J. H. Doonan and M. J. Hills: Endosperm defective 1 is a novel microtubule-associated protein essential for seed development in Arabidopsis. *Plant Cell*, 21, 90-105 (2009)

33. Segui-Simarro, J. M., J. R. Austin, 2nd, E. A. White and L. A. Staehelin: Electron tomographic analysis of somatic cell plate formation in meristematic cells of Arabidopsis preserved by high-pressure freezing. *Plant Cell*, 16, 836-856 (2004)

34. Nolasco, S., J. Bellido, J. Goncalves, J. C. Zabala and H. Soares: Tubulin cofactor A gene silencing in mammalian cells induces changes in microtubule cytoskeleton, cell cycle arrest and cell death. *FEBS Lett*, 579, 3515-3524 (2005)

35. Weingartner, M., M. C. Criqui, T. Meszaros, P. Binarova, A. C. Schmit, A. Helfer, A. Derevier, M. Erhardt, L. Bogre and P. Genschik: Expression of a nondegradable cyclin B1 affects plant development and

leads to endomitosis by inhibiting the formation of a phragmoplast. *Plant Cell*, 16, 643-657 (2004)

36. Weingartner, M., P. Binarova, D. Drykova, A. Schweighofer, J. P. David, E. Heberle-Bors, J. Doonan and L. Bogre: Dynamic recruitment of Cdc2 to specific microtubule structures during mitosis. *Plant Cell*, 13, 1929-1943 (2001)

Abbreviations: AtTFC B: Arabidopsis tubulin-folding cofactor B; PPB: preprophase band; GAP: GTPase-activating protein; Col: Columbia; ABRC: Arabidopsis Biological Resource Center; KIS: KIESEL; POR: PORCINO; TTN1: TITAN1; PFI: PFIFFERLING

Key Words: AtTFC B, Cell Division, Embryo, Microtubule, Nucleus

Send correspondence to: Yi Li, Peking-Yale Joint Center for Plant Molecular Genetics and Agrobiotechnology, National Laboratory of Protein Engineering and Plant Genetic Engineering, College of Life Science, The National Plant Gene Research Center, Peking University, Beijing 100871, China. National Center for Plant Gene Research, Beijing 100101, China, Tel: 86-10-62759690, Fax: 86-10-62756903, E-mail: liyi@ pku.edu.cn

http://www.bioscience.org/current/vol2E.htm